

1 **Fabrication of multi-well chips for spheroid cultures and implantable constructs**  
2 **through rapid prototyping techniques**

3 Silvia Lopa<sup>1,\$</sup>, Francesco Piraino<sup>2,\$</sup>, Raymond J. Kemp<sup>3</sup>, Clelia Di Caro<sup>2</sup>, Arianna B. Lovati<sup>1</sup>,  
4 Alessia Di Giancamillo<sup>4</sup>, Lorenzo Moroni<sup>3,5</sup>, Giuseppe M. Peretti<sup>4,6</sup>, Marco Rasponi<sup>2</sup>, Matteo  
5 Moretti<sup>1,\*</sup>

6 <sup>\$</sup> equally contributing authors

7 <sup>\*</sup> corresponding author

8

9 <sup>1</sup> Cell and Tissue Engineering Laboratory, IRCCS Galeazzi Orthopedic Institute, Via R. Galeazzi 4, 20161,  
10 Milan, IT

11 <sup>2</sup> Department of Electronics, Information and Bioengineering, Politecnico di Milano, Via Ponzio 34, 20133,  
12 Milan, IT

13 <sup>3</sup> University of Twente, Tissue Regeneration Department, Building Zuidhorst ZH 147, Drienerlolaan 5, 7522  
14 NB, Enschede, NL

15 <sup>4</sup> IRCCS Galeazzi Orthopedic Institute, Via R. Galeazzi 4, 20161, Milan, IT

16 <sup>5</sup> Maastricht University, Department of Complex Tissue Regeneration, PO Box 616, 6200 MD, Maastricht,  
17 NL

18 <sup>6</sup> Department of Biomedical Sciences for Health, Università degli Studi di Milano, Via L. Mangiagalli 31,  
19 20133, Milan, IT

20

21 **Corresponding author:**

22 Matteo Moretti

23 Cell and Tissue Engineering Laboratory, IRCCS Galeazzi Orthopedic Institute

24 Via R. Galeazzi, 4

25 20161 Milan, IT

26 Mail: [matteo.moretti@grupposandonato.it](mailto:matteo.moretti@grupposandonato.it)

27 Phone: +390266214049

28 Fax: +390266214060

29

30 **Running Title:**

31 Multi-well chips and constructs prototyping

32

33

1 **Abstract**

2 Three-dimensional culture models, such as cell spheroids, are widely used in basic and translational  
3 research. Since handling a high number of cell spheroids is more complex and time consuming than  
4 handling monolayer cultures, we exploited laser ablation and replica molding to fabricate  
5 polydimethylsiloxane (PDMS) multi-well chips for the generation and culture of multiple cell  
6 spheroids. Articular chondrocytes (ACs) were used to validate the multi-well PDMS chips. Multi-  
7 well spheroids were comparable or superior to standard spheroids in terms of chondrogenic  
8 differentiation. Moreover, the use of multi-well chips significantly reduced the operation time for  
9 cell seeding and medium refresh.

10 Using a similar approach, clinical-grade fibrin was used to generate implantable multi-well  
11 constructs, allowing differential cell seeding in the construct structure and in the wells. Multi-well  
12 fibrin constructs with high cell density regions were compared with constructs where ACs were  
13 homogeneously distributed. Expression of chondrogenic genes was increased after 7 days *in vitro* in  
14 both types of constructs, with multi-well constructs showing higher *SOX9* and *ACAN* levels than  
15 standard constructs. Through differential cell staining, we demonstrated that high cell density  
16 regions can be precisely generated in multi-well constructs and that they are still detectable after 5  
17 weeks *in vivo*.

18 In conclusion, multi-well chips for the generation and culture of multiple cell spheroids can be  
19 fabricated by low-cost rapid prototyping techniques. Furthermore, these techniques can be used to  
20 generate implantable constructs with defined architecture and spatially controlled cell distribution,  
21 allowing the *in vitro* and *in vivo* investigation of cell interactions in a 3D environment.

22

23 **Keywords**

24 Rapid prototyping, 3D model, Cell spheroid, Implantable scaffold, Tissue engineering

25

26

## 1 **Introduction**

2 Three-dimensional (3D) cultures are widely used as *in vitro* models for cell culture. Compared with  
3 monolayer cultures, 3D models better mimic the *in vivo* tissue features, thus providing a  
4 physiologically relevant environment (Abbott 2003). Among different types of 3D models  
5 developed in the last years, multiple cell aggregates or spheroids have been widely used in tumor  
6 (Burdett et al. 2010) and tissue engineering (Fennema et al. 2013) research areas. The screening of  
7 multiple drugs or culture conditions through 3D cell spheroids requires a relevant number of  
8 experimental replicates with cells from different donors, thus making the use of this 3D model more  
9 complex and time-consuming compared to conventional monolayer cultures. 3D spheroids,  
10 whereby specific extracellular matrix is produced by aggregated cells, also represent the living  
11 “building blocks” in organ printing, which aims at the layer-by-layer biofabrication of 3D  
12 functional tissues and organs (Boland et al. 2003; Jakab et al. 2004; Mironov et al. 2009).

13 The need to generate cell spheroids in a high throughput fashion for cancer research and for basic  
14 and translational tissue engineering studies has encouraged the development of multi-well devices  
15 as an alternative to standard methods for the formation and culture of multiple 3D cell spheroids  
16 (Babur et al. 2013; de Ridder et al. 2000; Moreira Teixeira et al. 2012; Ratnayaka et al. 2013).  
17 Indeed, these devices provide a relevant tool to implement 3D spheroid models, reducing the time  
18 required for routine operations and minimizing differences between experimental replicates.

19 Rapid prototyping techniques represent an exceptional tool to generate easy-handling platforms for  
20 3D cell culture. However, existing lithography-based approaches are often expensive and time  
21 consuming (Whitesides et al. 2001). Indeed, current approaches based on lithographic fabrication  
22 require cleanroom facilities where any minor change in the design involves increasing costs related  
23 to the fabrication process. Laser fabrication techniques offer an alternative to lithography-based  
24 approaches for rapid prototyping (Becker and Gartner 2008) and have been recently exploited for  
25 the fabrication of micro-wells in order to minimize fabrication complexity (Napolitano et al. 2007;  
26 Piraino et al. 2012; Selimovic et al. 2011).

1 Another key element for developing innovative 3D models is the possibility of generating scaffolds  
2 with a controlled micro- and/or macro-scale architecture , directing cell distribution and/or cell  
3 orientation by topographical cues (Bae et al. 2014; Gerberich and Bhatia 2013). Implantable multi-  
4 well scaffolds have recently been proposed for the *in vivo* evaluation of the influence of different  
5 extracellular matrix components on the differentiation of cells seeded within the wells (Higuera et  
6 al. 2013), demonstrating the great potentiality of this approach.

7 In this study we exploited laser ablation and replica molding to fabricate multi-well  
8 polydimethylsiloxane (PDMS) chips for the culture of multiple cell spheroids, using human  
9 articular chondrocytes (ACs) for their validation. ACs are widely investigated in the field of  
10 cartilage tissue engineering. Their re-differentiation, necessary to re-acquire their original  
11 phenotype after *in vitro* expansion (Giannoni and Cancedda 2006; Giannoni et al. 2005; Schulze-  
12 Tanzil 2009), is traditionally performed in 3D conditions (Bernstein et al. 2009; Dehne et al. 2010;  
13 Jakob et al. 2001; Zhang et al. 2004), indicating that this cell population is a suitable cell source for  
14 the validation of platforms for 3D spheroid formation and culture.

15 The same rapid prototyping techniques were used to biofabricate implantable fibrin multi-well  
16 constructs, allowing differential cell seeding into the construct structure and into the wells. We used  
17 a clinical-grade fibrin glue (Ahmed et al. 2008; Ahmed and Hincke 2010; Colombini et al. 2014a;  
18 Scotti et al. 2010) to validate our biofabrication process and through differential cell staining we  
19 verified the feasibility of precise cell seeding in different regions of the multi-well construct. As a  
20 proof of concept, we biofabricated fibrin constructs whereby human ACs were homogeneously  
21 dispersed or where different cell density regions were generated. Then, we evaluated cell behavior  
22 in standard and multi-well fibrin constructs after 1 and 7 days of *in vitro* culture and after 5 weeks  
23 of subcutaneous implantation in nude mice.

24

## 25 **Materials and Methods**

### 26 **Cell isolation and expansion**

1 Samples of articular cartilage were harvested from patients affected by osteoarthritis undergoing  
2 total hip replacement (5 males and 5 females, mean age  $64\pm 8$  years), with patients' informed  
3 written consent and with the approval of the Institutional Review Board. ACs were isolated from  
4 cartilage by enzymatic digestion using 0.15% type II collagenase (Worthington Biochemical Co)  
5 for 22 h at  $37^{\circ}\text{C}$ , according to a previously established protocol (Lagana et al. 2014; Lopa et al.  
6 2013). The cells were plated at a density of  $10^4$  cells/cm<sup>2</sup> and cultured in expansion medium.  
7 Expansion medium was composed as follows: High Glucose Dulbecco's Modified Eagle's Medium  
8 (HG-DMEM, Gibco) supplemented with 10% Fetal Bovine Serum (FBS, Lonza), 1% HEPES  
9 (Gibco), 1% Sodium pyruvate (Gibco), 1% Penicillin/Streptomycin/Glutamine (Gibco), 1 ng/mL  
10 Transforming Growth Factor  $\beta$ -1 (TGF- $\beta$ 1, Peprotech) and 5 ng/mL Fibroblast Growth Factor 2  
11 (FGF-2, Peprotech). At subconfluence, cells were detached by 0.05% trypsin/0.53 mM EDTA  
12 (Gibco) and plated at  $5\times 10^3$  cells/cm<sup>2</sup> for further expansion. At passage 2, cells were frozen and  
13 stored in liquid nitrogen. When needed, cells were thawed and expanded for one additional passage.  
14 To limit the expansion phase required to obtain a suitable number of cells, cells from different  
15 donors were pooled together to perform the experiments.

16

## 17 **Multi-well PDMS chips**

### 18 ***Fabrication of PMMA templates and multi-well PDMS chips***

19 Drawings of PMMA master templates were made by *AutoCAD*<sup>®</sup> software (<sup>©</sup>*Autodesk, Inc.*) and  
20 processed by *Corel*<sup>®</sup> *DRAW*<sup>TM</sup> software (<sup>©</sup>*Corel Corporation, 2002*). Master templates were  
21 obtained by carbon dioxide (CO<sub>2</sub>) laser ablation of a polymethylmethacrylate (PMMA) substrate  
22 (Fig. 1a, step I) in single hole drilling mode, as previously described (Piraino et al. 2012; Selimovic  
23 et al. 2011). The laser power was set at 22.5 W, the write speed at 0.08 mm/s, and  $z = 17.2$  mm  
24 (VLS2.30, VersaLASER). Substrate removal through ablation produced features with a Gaussian-  
25 profile. A PDMS mixture (Sylgard<sup>®</sup> 184, Dow Corning) was prepared at a 10:1 ratio  
26 (prepolymer/curing agent), degassed, poured on the PMMA master template, and baked at  $70^{\circ}\text{C}$  for

1 2h (Fig. 1a, step II). Once polymerized, the PDMS was carefully peeled off the PMMA master  
2 template and cleaned with 70% EtOH. After rinsing with ddH<sub>2</sub>O, PDMS multi-well chips were  
3 sterilized by autoclave.

4 Two different configurations of PDMS multi-well chips were designed to host 19 wells in a single  
5 chip. Features of the two multi-well chip configurations, named Chip A and Chip B, and their 3D  
6 renderings are reported respectively in Fig. 1b and 1c.

### 7 ***Cell spheroid formation***

8 Sterile PDMS chips were placed in a 12 well multiwell plate and each PDMS chip was seeded with  
9 a total number of  $2.85 \times 10^6$  cells by pipetting  $1.5 \times 10^5$  cells in each single well (Fig. 1a, step III). The  
10 12 well multiwell plate was then centrifuged for 5 min at 230g to favor spheroid formation. After 2  
11 h, 2.85 mL of chondrogenic medium were gently added to each well (Fig. 1a, step IV). Control  
12 (Ctrl) spheroids were prepared in 1.5 ml screw-cap conical tubes. Briefly,  $1.5 \times 10^5$  cells were  
13 suspended in 150  $\mu$ L of chondrogenic medium, transferred to a tube, and centrifuged for 5 min at  
14 230g. Chondrogenic medium was composed as follows: HG-DMEM supplemented with 0.029  
15 mg/ml L-glutamine, 100 U/ml penicillin, 100  $\mu$ g/ml streptomycin, 10 mM HEPES, 1 mM sodium  
16 pyruvate, 1.25 mg/ml Human Serum Albumin (HSA, Sigma-Aldrich), 1% ITS+1 (containing 1.0  
17 mg/ml insulin from bovine pancreas, 0.55 mg/ml human transferrin, 0.5  $\mu$ g/ml sodium selenite, 50  
18 mg/ml bovine serum albumin and 470  $\mu$ g/ml linoleic acid, Sigma-Aldrich), 0.1  $\mu$ M dexamethasone,  
19 0.1 mM L-ascorbic acid-2-phosphate and 10 ng/ml TGF- $\beta$ 1. Samples were cultured for 21 days  
20 (37°C, 5% CO<sub>2</sub>). Medium was replaced twice per week.

### 21 ***Measurement of operation time for cell seeding and medium refresh***

22 For spheroid culture in standard tubes and in multi-well PDMS chips, we measured the operation  
23 time required to perform cell seeding and medium refresh. Independent measures were obtained  
24 testing 3 operators with different skill levels in cell culture techniques.

### 25 ***Spheroid analysis***

#### 26 *Evaluation of spheroid area*

1 After 7, 14, and 21 days of culture in chondrogenic medium, spheroids in the multi-well chips were  
2 photographed to monitor the size variation. Spheroid area was determined by image analysis using  
3 ImageJ software.

#### 4 *Quantification of metabolic activity and DNA content*

5 After 21 days of culture in chondrogenic medium, cell metabolic activity was evaluated by Alamar  
6 Blue assay. Briefly, spheroids were randomly harvested from different PDMS chips and from the  
7 tubes (control group), transferred to a 96 well multiwell plate, and incubated with 100  $\mu$ L HG-  
8 DMEM supplemented with 10% Alamar Blue for 4 h at 37°C. After incubation, the supernatant was  
9 harvested and fluorescence was measured (540 nm-580 nm) using a Victor X3 Plate Reader (Perkin  
10 Elmer). The same spheroids were lysed for DNA quantification. After washing with Phosphate  
11 Buffered Saline (PBS), spheroids were digested (16 h, 60°C) in 500  $\mu$ l of PBE buffer (100 mM  
12  $\text{Na}_2\text{HPO}_4$ , 10 mM NaEDTA, pH 6.8) containing 1.75 mg/ml L-cystein (Sigma-Aldrich) and 14.2  
13 U/ml papain (Worthington). DNA quantification was performed by CyQUANT Kit (Invitrogen),  
14 according to the manufacturer's instructions.

#### 15 *Histological and immunohistochemical analysis*

16 For histological analysis, chondrocyte spheroids cultured for 21 days were fixed for 24 h in 10%  
17 neutral buffered formalin, embedded in paraffin and sectioned at 3  $\mu$ m. Sections were stained with  
18 alcian blue (pH 2.5, Sigma-Aldrich) to detect glycosaminoglycans (GAGs). For  
19 immunohistochemistry, sections were deparaffinized, rehydrated, and treated with 3% hydrogen  
20 peroxide in distilled water for 15 min. Mouse monoclonal anti-Collagen II antibody (SPM239,  
21 ab54236, Abcam) was applied at room temperature for 1 h. The sections were labeled by the avidin-  
22 biotin-peroxidase (ABC) procedure (Hsu et al. 1981) with a commercial immunoperoxidase kit  
23 (Vectastain Standard Elite; Vector Laboratories). The immunohistochemical reaction was  
24 developed with 3.3' diaminobenzidine (DAB) for 5 min and sections were counterstained for 2 min  
25 with Mayer's hematoxylin.

26

## 1 **Implantable multi-well fibrin constructs**

### 2 *Fabrication of PMMA master templates and PDMS counter-molds*

3 PMMA master templates and the corresponding PDMS counter-molds were fabricated by CO<sub>2</sub> laser  
4 ablation (Fig. 2a, step I) and replica molding (Fig. 2a, step II), as previously described for the  
5 fabrication of multi-well PDMS chips.

6 Three different configurations of PDMS molds were designed to biofabricate fibrin constructs with  
7 multi-well bottom layers containing 19, 10, or 7 wells (Fig. 2b). Features of the three different  
8 PDMS mold configurations, named Mold X, Mold Y, and Mold Z, and their 3D renderings are  
9 reported respectively in Fig. 2b and 2c. Immediately prior to use, PDMS molds were plasma treated  
10 (Harrick Plasma Instruments, USA) for 8 minutes to reduce surface hydrophobicity.

### 11 *Biofabrication of multi-well fibrin constructs*

12 The two-component fibrin sealant Tisseel<sup>®</sup> (Baxter Biosurgery) was used to generate the fibrin  
13 constructs. The fibrinogen component contained 91 mg/mL human fibrinogen and 3000 KIU/mL  
14 aprotinin solution. The thrombin component was diluted to 5 U/mL in 40 mM of CaCl<sub>2</sub> at pH 7.0.  
15 Initially, fibrin constructs with three different configurations of the multi-well bottom layer were  
16 prepared according to the protocol depicted in Fig. 2a: (X) 19 wells,  $\varnothing_{\text{well}}$  1 mm,  $h_{\text{well}}$  1.5 mm; (Y)  
17 10 wells,  $\varnothing_{\text{well}}$  1.5 mm,  $h_{\text{well}}$  1.5 mm; (Z) 7 wells,  $\varnothing_{\text{well}}$  2 mm,  $h_{\text{well}}$  1.5 mm. For each construct,  
18  $1.15 \times 10^6$  cells were suspended in fibrinogen and thrombin mixed at a 1:1 ratio (cell density  
19  $15.4 \times 10^6$  cells/mL) and poured into the PDMS molds until polymerization (1 h, 37°C, Fig. 2a, step  
20 III). The bottom layer was then gently removed from the PDMS mold and transferred into a 12 well  
21 multiwell plate. Custom made PDMS rings ( $\varnothing_{\text{out}}$  10 mm,  $\varnothing_{\text{in}}$  8 mm, h 3 mm) were placed around  
22 the bottom layers. Then, different cell numbers were seeded in each well, depending on the  
23 construct configuration (Fig. 2a, step IV): (X)  $1 \times 10^5$  cells in  $\varnothing_{\text{well}}$  1 mm; (Y)  $2 \times 10^5$  cells in  $\varnothing_{\text{well}}$  1.5  
24 mm; (Z)  $4 \times 10^5$  cells in  $\varnothing_{\text{well}}$  2 mm. After 15 minutes, a fibrin top layer ( $\varnothing$  8 mm, h 1 mm) was  
25 generated by suspending  $8.5 \times 10^5$  cells with fibrinogen and thrombin mixed at a 1:1 ratio (cell  
26 density  $15.4 \times 10^6$  cells/mL) and pouring the mixture over the multi-well bottom layer (Fig. 2a, step



1 V). In this phase, the PDMS ring was used to match the bottom layer shape and to avoid fibrin  
2 leaking. After polymerization, the PDMS ring was removed and constructs were cultured in 3 mL  
3 chondrogenic medium (Fig. 2a, step VI). After selecting the best bottom layer configuration based  
4 on the reproducibility of construct fabrication and cell seeding into the wells, we compared the  
5 multi-well fibrin constructs (10 wells,  $\varnothing_{\text{well}}$  1.5 mm,  $h_{\text{well}}$  1.5 mm,  $2 \times 10^5$  cells/well) with a similar  
6 construct without wells. Both types of fibrin constructs ( $\varnothing$  8 mm, h 3 mm) were seeded with a total  
7 number of  $4 \times 10^6$  cells. Bottom and top layer of the multi-well fibrin constructs were prepared as  
8 aforementioned. To seed the wells of the constructs, a cell suspension with a density of  $10^8$  cells/mL  
9 was prepared. In each well, we added 2  $\mu\text{L}$  of solution, corresponding to  $2 \times 10^5$  cells. To prepare  
10 standard fibrin constructs without wells,  $4 \times 10^6$  cells were suspended in fibrinogen and thrombin  
11 mixed at a 1:1 ratio (cell density  $26.7 \times 10^6$  cells/mL). The mixture was poured into the custom made  
12 PDMS rings and let polymerize for 1 h at  $37^\circ\text{C}$ . After polymerization, all constructs were cultured  
13 in 3 mL chondrogenic medium.

#### 14 ***Fibrin construct analysis***

##### 15 *Evaluation of multi-well structure and cell distribution*

16 The macroscopic features of the different bottom layers were evaluated by stereomicroscope  
17 (Olympus SXZ10). Cell distribution into the construct and feasibility of cell seeding into the wells  
18 were evaluated by fluorescence microscopy (Olympus IX71) using green- or red- cells stained  
19 either with the green fluorescent dye Vybrant DiO or with the red fluorescent dye Vybrant CM-Dil  
20 (both from Invitrogen) according to the manufacturer's instructions. Briefly, after trypsinization  
21 cells were suspended at a density of  $1 \times 10^6$  cells/mL in serum-free culture medium. Vybrant DiO or  
22 Vybrant CM-Dil was added to the cell suspension (5  $\mu\text{L}/\text{mL}$ ). Cells were incubated for 10 min at  
23  $37^\circ\text{C}$  and then centrifuged (350g, 5 min). The supernatant was removed and the cells were washed  
24 twice in expansion medium prior to use.

##### 25 *Histological analysis*

1 After 7 days of *in vitro* culture, fibrin constructs cultured for 7 days were fixed for 24 h in 10%  
2 neutral buffered formalin, embedded in paraffin and sectioned at 3  $\mu$ m. For morphological  
3 evaluation of fibrin glue constructs, sections were stained with hematoxylin and eosin (HE).

#### 4 *Quantification of DNA and GAGs content*

5 After 7 days of *in vitro* culture, fibrin constructs were digested, as previously described for  
6 chondrocyte spheroids. DNA quantification was performed by CyQUANT Kit. The amount of  
7 GAGs was spectrophotometrically measured using 16 mg/mL dimethylmethylene blue (Sigma-  
8 Aldrich), with chondroitin sulphate as standard (absorbance 525 nm) (Lopa et al. 2014). GAGs  
9 content was normalized to the DNA content and expressed as  $\mu$ g GAGs/ $\mu$ g DNA.

#### 10 *Gene expression analysis*

11 After 1 and 7 days of *in vitro* culture, fibrin constructs were harvested and stored in liquid nitrogen  
12 for RNA isolation and gene expression analysis. Total RNA was purified using RNeasy Mini kit  
13 (Qiagen) following sample disruption with TissueRuptor (Qiagen). RNA was quantified using a  
14 spectrophotometer (Nanodrop, Thermo Scientific) and reverse-transcribed to cDNA using iScript  
15 cDNA Synthesis Kit (Bio-Rad Laboratories). Gene expression was evaluated by real time PCR  
16 (StepOne Plus, Life Technologies). 40 ng of cDNA were incubated with a PCR mixture including  
17 TaqMan<sup>®</sup> Universal PCR Master Mix and TaqMan<sup>®</sup> Assays-on-Demand<sup>™</sup> Gene expression probes  
18 (Life Technologies) using the following assays: glyceraldehyde-3-phosphate dehydrogenase  
19 (*GAPDH*, Hs99999905\_m1), SRY (Sex determining region Y)-box9 (*SOX9*, Hs00165814\_m1),  
20 collagen type II alpha I (*COL2A1*, Hs00264051\_m1), aggrecan (*ACAN*, Hs00153936\_m1), and  
21 cartilage oligomeric matrix protein (*COMP*, Hs00164359\_m1) The expression of the analyzed  
22 markers was normalized to *GAPDH* using the delta Ct method.

#### 23 *Subcutaneous implantation of fibrin constructs in nude mice*

24 Fibrin constructs without or with wells were seeded with green- and red-stained cells and  
25 subcutaneously implanted in nude mice. The *in vivo* study was approved by the Mario Negri  
26 Institute for Pharmacological Research (IRFMN) Animal Care and Use Committee (IACUC).

1 Animals and their care were handled in compliance with institutional guidelines as defined in  
2 national (Law 116/92, Authorization n.19/2008-A issued March 6, 2008, Italian Ministry of Health)  
3 and international laws and policies (EEC Council Directive 86/609, OJ L 358. 1, December 12,  
4 1987; Standards for the Care and Use of Laboratory Animals - UCLA, U.S. National Research  
5 Council, Statement of Compliance A5023-01, November 6, 1998).

6 Three 6-week-old female athymic mice were obtained from Harlan® and maintained in the Animal  
7 Care Facilities of the IRFMN, under specific pathogen-free conditions with food and water  
8 provided *ad libitum*. Animals were anesthetized by intraperitoneal injection of ketamine chloride  
9 (80 mg/kg, Imalgene, Merial) and medetomidine hydrochloride (1 mg/kg, Domitor, Pfizer).  
10 Surgical procedures were performed in sterile conditions under a laminar flow hood. Four  
11 subcutaneous pockets were created on the dorsum of each mouse by blunt dissection through cranial  
12 and caudal skin incisions. One fibrin construct was inserted in each pocket, then the skin was  
13 sutured with #4-0 Monocryl thread (Ethicon). After 5 weeks, mice were euthanized by CO<sub>2</sub>  
14 inhalation and constructs were explanted.

### 15 ***Explant analysis***

#### 16 *Evaluation of cell distribution*

17 After 5 weeks in vivo, the distribution of green- and red- stained cells in the explants was evaluated  
18 by fluorescent microscopy (Olympus IX71).

#### 19 *Quantification of GAGs content*

20 Fibrin constructs cultured in vitro for 7 days were analyzed before and after *in vivo* subcutaneous  
21 implantation for 5 weeks. Samples were digested in PBE buffer and GAGs were quantified by  
22 dimethylmethylene blue assay, as aforementioned. GAGs content was normalized to the construct  
23 wet weight (mg).

24

### 25 **Statistical analysis**

1 All data are presented as mean±SD. Kolmogorov-Smirnov test was used to assess the normal data  
2 distribution (GraphPad Prism version 5.00 for Windows, GraphPad Software). For spheroid  
3 analysis, comparison among the three different experimental groups (control spheroids, spheroids in  
4 chip A, spheroids in chip B) was performed by One-Way ANOVA with Dunnett's post hoc-test.  
5 Mann-Whitney test (unpaired data) for non-normally distributed data was performed to compare  
6 different types of fibrin constructs at the same time point (i.e. w/ wells 1d vs. w/o wells 1d) and to  
7 compare the same type of fibrin construct at different time points (i.e. w/ wells 1d vs. w/ wells 7d).

8

## 9 **Results**

### 10 **Multi-well PDMS chips support the generation and culture of chondrocyte spheroids**

11 Multi-well chips were generated by PDMS replica molding on a laser-ablated PMMA master  
12 templates. Optical images of the fabricated multi-well PDMS chips in figure 1d show the fidelity of  
13 the multi-well arrays to the original design. As expected, the side view of the PDMS chips section  
14 revealed the conical shape of the wells (Fig. 1d, bottom panel).

15 Articular chondrocytes were used to validate the multi-well PDMS chips as devices for the  
16 formation and culture of 3D cell spheroids. The PDMS chips were designed to fit the wells of a 12  
17 multiplate, allowing the simultaneous culture of several spheroids in different experimental  
18 conditions in the same plate, as shown in figure 3a, where PDMS chips immediately after cell  
19 seeding are depicted. The use of these devices significantly reduced the time required for cell  
20 seeding and medium refresh operations compared to standard spheroid culture, representing a  
21 technical amelioration in terms of work efficiency (Fig. 3b,c). The PDMS chips, thanks to the  
22 transparency of the material, also allowed us to monitor the samples through microscopy over the  
23 entire period of culture and to measure basic parameters, such as spheroid area. As shown in figure  
24 3d, cell aggregates started to form already 24 hours after cell seeding and, after 21 days of culture,  
25 spheroids were well-formed in both PDMS chips. Spheroid area increased from 7 to 21 days of  
26 chondrogenic culture due to matrix deposition (Fig. 3e). At the end of culture, we compared the

1 metabolic activity of spheroids cultured in standard tubes (Ctrl) and in PDMS chips. No significant  
2 difference in metabolic activity was observed among the experimental groups (Fig. 3f). In the same  
3 way, the DNA content and the metabolic activity normalized on DNA of spheroids cultured in  
4 standard tubes and in PDMS chips did not differ, showing that spheroids cultured in PDMS chips  
5 were at least as viable and active standard spheroids (Fig. 3g,h). Histological evaluation revealed  
6 that GAGs deposition, which is a key marker of chondrogenic differentiation, was comparable in  
7 Ctrl spheroids and in spheroids cultured in multi-well PDMS chips (Fig. 3i). Lacunar structures,  
8 similar to those found in native hyaline cartilage, were observed in all the experimental groups.  
9 Analysis of type II collagen deposition by immunohistochemistry displayed a more intense staining  
10 in spheroids cultured in PDMS chips compared to standard spheroids, indicating the production of  
11 highly specialized extracellular matrix in these samples (Fig. 3j).

12

### 13 **Implantable multi-well fibrin constructs with high cell density regions support the 3D culture** 14 **and re-differentiation of articular chondrocytes**

15 Multi-well fibrin glue constructs were prepared according to the scheme in Fig. 1b. The simplicity  
16 of the biofabrication process allowed us to prepare 65 multi-well constructs in a single experimental  
17 run. PMMA master templates and PDMS molds with the three different configurations (X, Y, Z)  
18 were used to generate the corresponding bottom layers (Fig. 4a). We noticed that the configuration  
19 with 10 wells ( $\text{\O}_{\text{well}}$  1.5 mm) was the easiest to fabricate and handle. Indeed, the configuration with  
20 larger wells ( $\text{\O}_{\text{well}}$  2 mm) had a very thin outer border that did not allow for the easy removal of the  
21 construct from the PDMS mold. The peripheral border of these constructs tended to break during  
22 this operation (Fig. 4a, upper row), resulting in leaking of the seeded cells into the adjacent wells.  
23 On the other hand, the configuration with smaller wells ( $\text{\O}_{\text{well}}$  1 mm) was quite easy to manipulate  
24 since stiffer, but small imperfections in the fibrin bottom layer resulted in a dramatic reduction of  
25 the volume of the wells (Fig. 4a, upper row), which challenged the reproducibility of cell seeding.  
26 Cell embedding in the bottom layer resulted in a homogeneous cell distribution (Fig. 4b, upper row,

1 green-stained cells) and cell seeding in the multi-wells proved also to be effective (Fig. 4b, middle  
2 and lower row). Based on the aforementioned considerations about simplicity and reproducibility of  
3 fabrication, we selected the configuration (Y) with 10 wells ( $\varnothing_{\text{well}}$  1.5 mm,  $h_{\text{well}}$  1.5 mm) for the  
4 prosecution of the study. The central section of the bottom layer shows the cell deposition on the  
5 bottom side of each well (Fig. 4c), demonstrating that red-stained cells were confined into the wells  
6 and that we were able to generate regions with different cell density in a single construct. The multi-  
7 well constructs were completed by adding the top layer, as shown in figure 4d, where the multi-well  
8 array in the finalized scaffold can be observed.

9 In figure 5a, macroscopic pictures of fibrin constructs without and with wells show that the pattern  
10 of multi-wells was still visible under the top layer (right image). In fibrin constructs without wells,  
11 cells were homogeneously distributed throughout the entire scaffold (Fig. 5b,c, left image), whereas  
12 in multi-well constructs single wells were clearly visible and hematoxylin/eosin staining showed  
13 that a cell multi-layer was present in the wells (Fig. 5b,c, right image), demonstrating once again  
14 that different cell density areas were generated in the construct. As revealed by histological  
15 analysis, poor matrix deposition and construct remodeling occurred after 7 days of *in vitro* culture  
16 (Fig. 5c), probably due to the high concentration of fibrinogen used in our constructs as well as to  
17 the short period of *in vitro* culture.

18 After 7 days of culture in chondrogenic medium, the same number of cells was found in fibrin  
19 constructs without and with wells (Fig. 5d) and no significant difference in terms of GAGs content  
20 per cell between the two types of fibrin constructs was observed (Fig. 5e). Gene expression analysis  
21 performed after 1 and 7 days of culture in chondrogenic medium revealed that both types of fibrin  
22 constructs well supported chondrocyte re-differentiation. Indeed, we observed that levels of  
23 chondrogenic markers such as *SOX9*, *COL2A1*, *ACAN*, and *COMP* increased from day 1 to day 7,  
24 with significant differences between time points for all the analyzed markers with the exception of  
25 *SOX9* (Fig. 5f-i). Higher transcriptional levels of all the tested markers were measured in ACs

1 cultured in fibrin constructs with high cell density regions for 7 days, albeit increases with respect  
2 to constructs without wells were not significantly different (Fig. 5f-i).

3 Finally, we evaluated the *in vivo* behavior of ACs in fibrin constructs without or with wells through  
4 subcutaneous implantation in nude mice. After 5 weeks of implantation, construct size was  
5 dramatically reduced. The pictures reported in Fig. 6a represent the same constructs imaged before  
6 and after *in vivo* implantation with the same microscope magnification, clearly showing the  
7 diameter reduction from 8 mm to 1.5-2 mm. Surprisingly, despite the reduction in construct size,  
8 the multi-well structure was maintained, as shown in the post-implantation pictures where the high  
9 cell density areas corresponding to the wells are still visible. GAGs content was evaluated in the  
10 fibrin constructs cultured *in vitro* for 7 days (pre-implantation) and in the explants harvested after 5  
11 weeks of subcutaneous implantation (post-implantation). The content of GAGs normalized on  
12 construct wet weight was found to be significantly increased in both types of fibrin constructs after  
13 5 weeks *in vivo*, with no significant differences between the two types of fibrin constructs at any  
14 time point (Fig. 6b).

15

## 16 **Discussion**

17 The primary purpose of this study was to generate multi-well PDMS chips supporting the formation  
18 and culture of cell spheroids and to biofabricate a multi-well fibrin construct through low-cost and  
19 easily accessible rapid prototyping techniques.

20 Compared to standard protocols, the use of the PDMS multi-well chips significantly reduced the  
21 operation time for cell seeding and medium refresh, which are highly time-consuming factors when  
22 preparing several experimental replicates and working with many experimental groups. The  
23 possibility to culture simultaneously a maximum of 228 cell spheroids in a single 12 well multiwell  
24 plate also reduced the space required for the culture of such a high number of samples in the CO<sub>2</sub>  
25 incubator. Furthermore, the optical transparency of the PDMS chips allowed us to monitor the

1 process of spheroid formation and the changes in dimension and shape occurring during culture.  
2 The high hydrophobicity of PDMS (Berthier et al. 2012), related to the low cell adhesion on this  
3 material, led to the formation of well-defined chondrocyte spheroids in both the tested  
4 configurations. The comparison between spheroids generated and cultured in PDMS chips with  
5 spheroids in polypropylene tubes did not show any significant difference in terms of cell  
6 proliferation and metabolic activity. On the contrary, while deposition of GAGs was similar in the  
7 different experimental groups, type-II collagen was more present in spheroids cultured in the PDMS  
8 chips compared to standard spheroids. These results indicate that the multi-well devices were able  
9 to support very well both cell viability and chondrogenic differentiation, thus representing an  
10 appealing option for 3D cell culture. A similar approach has been used in a very recent study to  
11 produce and culture chondrocyte micro-pellets (166 cells/pellet) by Babur and co-workers (Babur et  
12 al. 2013). In their study, the PDMS insert surface had to be chemically modified to avoid cell  
13 spreading all over the well. By contrast, in our devices the higher ratio between the number of  
14 plated cells and the surface available for cell growth overcame the need for any chemical surface  
15 treatment, since centrifugation was sufficient to trigger spheroid formation in the wells. Rapid  
16 prototyping of PDMS devices hold great potential for studies requiring the indirect co-culture of  
17 different cell types, as previously reported for hepatocytes and Kupffer cells (Zinchenko and Coger  
18 2005). In our system, the possibility to precisely seed each well with a specific cell population,  
19 together with the easiness of spheroid harvesting from selected wells, allows to evaluate the effect  
20 of paracrine factors in each cell type, representing a complementary alternative to the trans-well  
21 system where cells are traditionally cultured in monolayer. A major limitation in the use of the  
22 presented multi-well devices may be represented by the high hydrophobicity and porosity of PDMS  
23 which may cause the nonspecific absorption of small molecules and hence bias the biological  
24 outcomes in cell culture applications (Toepke and Beebe 2006). In our multi-well system, to  
25 maintain stable cell culture conditions and to reduce the effects of nonspecific absorption into  
26 PDMS, we performed systematic replacement of culture medium. Indeed, we did not observe any



1 negative effect on the re-differentiation of ACs cultured in multi-well PDMS chips compared to  
2 spheroids cultured in standard polypropylene tubes. However, since in the last years a number of  
3 surface treatments have been developed to prevent nonspecific absorption of molecules, such as sol-  
4 gel chemistry (Gomez-Sjoberg et al. 2010) or pre-treatment with n-dodecyl- $\beta$ -D-maltoside (Huang  
5 et al. 2005), or polyethylene glycol and N-acetyl-L-cysteine (Harris et al. 2011) we envision in the  
6 future to pre-treat our PDMS devices to minimize possible bias in studies evaluating the paracrine  
7 interaction between multiple cell types. Besides applications in basic research investigating the  
8 mutual influence between different cell types, multi-well PDMS chips can be used to produce a  
9 high number of mini-tissue spheroids, which represent the building blocks in organ printing  
10 approaches (Boland et al. 2003; Jakab et al. 2004; Mironov et al. 2009). Indeed, we found that  
11 spheroids were viable and metabolically active after a relatively long culture period and histological  
12 evaluation showed that cells were able to produce specific extracellular matrix. Finally, considering  
13 the field of cartilage tissue engineering, the low-cost multi-well PDMS chips described here could  
14 be exploited to generate a high number of autologous 3D chondral spheroids to be used in the  
15 treatment of chondral defects, as proposed by a recent clinical trial (<http://clinicaltrials.gov/>,  
16 NCT01222559).

17 Here, to generate cell spheroids we exploited low-cost rapid prototyping techniques to fabricate  
18 multi-well PDMS chips and we took advantage of centrifugal force to promote cell assembly into  
19 3D spheroids. More complex systems can also be implemented. For example, cell spheroids can be  
20 generated within microfluidic devices combining the actions of fluid flow and gravity force,  
21 whereby cell trapping can be controlled modulating flow rate, cell density and seeding time (Fu et  
22 al. 2014; Patra et al. 2013). Alternatively, multiple cell spheroids can be generated using hanging  
23 drop plates which rely on gravity-enforced cell assembly (Cavnar et al. 2014; Tung et al. 2011).  
24 This method has been recently combined with the bioprinting approach to generate uniform-sized  
25 embryoid body replacing manual pipetting with the automated printing of single cells and  
26 exploiting the gravity force to induce cell assembly (Xu et al. 2011). All these methods represent

1 have advantages and disadvantages and require a preliminary optimization phase, which is more or  
2 less extensive depending on the easiness of the system. Anyhow, the growing body of literature in  
3 this field is a clear indication of the wide number of applications whereby cell spheroids can be  
4 used both as 3D models or as tissue building blocks.

5 In the second part of the study, we applied the same rapid prototyping techniques to produce a  
6 multi-well implantable fibrin construct. Considering the field of cartilage tissue engineering, we  
7 suggest that a similar configuration can be used to generate high cell density areas within the  
8 construct, leading to the formation of “chondrogenic centers” able to promote the differentiation of  
9 low cell density regions. Indeed, it has been shown that cell density affects the capability of  
10 chondrocytes to produce specific matrix and that a high cell density improves cartilaginous matrix  
11 deposition in 3D scaffolds (Mauck et al. 2003; Talukdar et al. 2011). Since cartilage biopsies  
12 harvestable from patients are limited in size and allow the retrieval of a limited number of  
13 chondrocytes, an extensive *in vitro* expansion phase is required to obtain enough cells to seed a 3D  
14 scaffold with a high cell density, which implies chondrocyte de-differentiation (Giannoni and  
15 Cancedda 2006; Giannoni et al. 2005; Schulze-Tanzil 2009; Steinert et al. 2007). The possibility of  
16 limiting the high cell density to some construct regions, acting as “chondrogenic centers”, implies a  
17 reduction in the number of cells required to seed the construct, and subsequently a shorter  
18 expansion phase and a lower impact of cell de-differentiation. Similar approaches have been  
19 proposed by other groups that have used chondrocytes aggregates of different dimensions seeded  
20 either in a collagen porous scaffold (Wolf et al. 2008) or embedded in a hydrogel (Moreira Teixeira  
21 et al. 2012). Here, we did not generate the chondrocyte aggregate before, but high cell density  
22 centers were represented by confluent cell multilayers within the wells. We found that 3D culture in  
23 fibrin constructs supported the chondrogenic re-differentiation of articular chondrocytes, as  
24 demonstrated by gene expression analysis over time. Furthermore, we found that the presence of  
25 high cell density regions in the fibrin constructs improved the transcriptional expression of  
26 chondrogenic markers such as *SOX9* and *ACAN*, which encode respectively for a transcriptional

1 factor modulating the chondrogenic cascade and for one of the major components of cartilaginous  
2 extracellular matrix, supporting the hypothesis that high cell density regions may act as  
3 chondrogenic centers; however, the short period of *in vitro* culture did not allow us to appreciate  
4 possible differences in terms of extracellular matrix deposition.

5 Remarkably, the construct configurations proposed here also offer the flexibility to be seeded with  
6 pre-formed cell aggregates where desired, being the dimensions of the wells compatible with those  
7 of chondrocyte spheroids obtained through standard techniques ( $1.5 \times 10^5$ - $5 \times 10^5$  cells/spheroid). In  
8 this case, the use of multi-well constructs described here would allow the controlled distribution of  
9 cell aggregates which cannot be achieved through a randomized seeding.

10 As hypothesized for the PDMS chips, the multi-well construct produced in this study, can be used  
11 for the co-culture of different cell types that is usually performed by more standard 3D models such  
12 as spheroids (Giovannini et al. 2010; Lopa et al. 2013; Wu et al. 2012) and random cell dispersion  
13 in 3D scaffolds (Hildner et al. 2009; Sabatino et al. 2012). The controlled distribution of  
14 mesenchymal stem cells and bovine chondrocytes in an implantable multi-well scaffold has been  
15 performed in a recent study screening the effect of several extracellular matrix components on the  
16 chondrogenesis of MSCs co-cultured with bovine chondrocytes (Higuera et al. 2013). Differently  
17 from this screening platform where a polymeric scaffold is used and cells are seeded uniquely into  
18 the wells (Higuera et al. 2013), in our fibrin multi-well construct cells can be seeded both into the  
19 construct structure and in the wells, further allowing to evaluate the interactions among multiple  
20 cell types distributed in different construct regions.

21 Bioprinting techniques could be exploited as an alternative to the biofabrication approach employed  
22 here to control cell distribution in 3D fibrin constructs, as reported in a recent study where human  
23 endothelial cells and fibrin have been used as bio-ink for microvasculature construction (Cui and  
24 Boland 2009). Similarly to the biofabrication method that we have used in the present study, the  
25 bioprinting approach would be suitable for the generation of constructs seeded with multiple cell  
26 types (Kolesky et al. 2014; Schuurman et al. 2011). As demonstrated by several studies employing

1 bioprinting to generate complex 3D structures, this approach allows a precise control over construct  
2 configuration and cell distribution (Murphy and Atala 2014). However, differently from the easy  
3 biofabrication method that we have presented here, the implementation of bioprinting would require  
4 an extensive preliminary phase to establish the optimal concentration of fibrinogen, thrombin,  
5 CaCl<sub>2</sub> as well as the polymerization time to obtain the desired configuration and grant proper cell  
6 distribution and viability, representing a highly time-consuming phase in the biofabrication process.  
7 Regarding the behavior of fibrin constructs *in vivo*, we observed a dramatic size reduction of the  
8 implants after 5 weeks of subcutaneous implantation. This result has been previously reported in  
9 several short-term *in vivo* studies (Colombini et al. 2014b; Hwang et al. 2013; Peretti et al. 2000)  
10 and can be explained by two major features of fibrin: its tendency to shrink and its fast degradation  
11 rate (Ahmed et al. 2008; Meinhart et al. 1999; Wolbank et al. 2014). Thanks to fluorescent cell  
12 staining, we verified that the implant size reduction did not alter cell distribution. Indeed dispersed  
13 red-stained cells and green-stained spot corresponding to the high cell density regions were clearly  
14 visible before and after subcutaneous implantation. On the other hand, when fibrin constructs were  
15 cultured *in vitro* for 7 days we observed a poor construct remodeling, meaning that the multi-well  
16 structure was well preserved and that cells were not able to deposit a relevant amount of  
17 extracellular matrix. These observations can be explained by the short period of *in vitro* culture  
18 applied, sufficient to reveal an increase in the transcriptional expression of chondrogenic genes, but  
19 not a relevant deposition of matrix proteins, and by the high concentration of fibrinogen used in our  
20 fibrin glue formulation, further stabilized by the presence of aprotinin (Meinhart et al. 1999).  
21 Hence, since it has been shown that lower concentrations of fibrinogen are compatible with the  
22 biofabrication of patterned scaffolds (Koroleva et al. 2012), we envision to tune this parameter in  
23 future *in vitro* studies in order to favor the interaction of multiple cell types seeded in different  
24 construct regions as well as extracellular matrix deposition.

25

1 **Conclusions**

2 We have presented a cost-effective method exploitable for the fabrication of platforms for the  
3 culture of multiple cell spheroids and for scaffold prototyping. Remarkably, the proposed  
4 fabrication approach is simple and exploits economic tools, as commercial design software and  
5 desktop laser, which do not require dedicated facilities and are accessible to most research labs.  
6 These features prompting the application of this approach in basic and translational research,  
7 whereby cell spheroids and 3D constructs represent key models in drug screening studies as well as  
8 the building blocks for translational tissue engineering approaches.

9

10 **Acknowledgements**

11 This work was supported by the Italian Ministry of Health. The authors would like to acknowledge  
12 Alessandra Colombini, MSc and Cristina Ceriani, MSc for their precious help in the optimization of  
13 RNA isolation from fibrin constructs and in gene expression analysis.

14

15 **Disclosure**

16 Authors have no competing interests to declare

17

18

## 1 **References**

- 2 Abbott A. 2003. Cell culture: biology's new dimension. *Nature* 424(6951):870-2.
- 3 Ahmed TA, Dare EV, Hincke M. 2008. Fibrin: a versatile scaffold for tissue engineering applications. *Tissue*  
4 *Eng Part B Rev* 14(2):199-215.
- 5 Ahmed TA, Hincke MT. 2010. Strategies for articular cartilage lesion repair and functional restoration.  
6 *Tissue Eng Part B Rev* 16(3):305-29.
- 7 Babur BK, Ghanavi P, Levett P, Lott WB, Klein T, Cooper-White JJ, Crawford R, Doran MR. 2013. The  
8 interplay between chondrocyte redifferentiation pellet size and oxygen concentration. *PLoS One*  
9 8(3):e58865.
- 10 Bae CY, Min MK, Kim H, Park JK. 2014. Geometric effect of the hydrogel grid structure on in vitro formation  
11 of homogeneous MIN6 cell clusters. *Lab Chip* 14(13):2183-90.
- 12 Becker H, Gartner C. 2008. Polymer microfabrication technologies for microfluidic systems. *Anal Bioanal*  
13 *Chem* 390(1):89-111.
- 14 Bernstein P, Dong M, Corbeil D, Gelinsky M, Gunther KP, Fickert S. 2009. Pellet culture elicits superior  
15 chondrogenic redifferentiation than alginate-based systems. *Biotechnol Prog* 25(4):1146-52.
- 16 Berthier E, Young EW, Beebe D. 2012. Engineers are from PDMS-land, Biologists are from Polystyrenia. *Lab*  
17 *Chip* 12(7):1224-37.
- 18 Boland T, Mironov V, Gutowska A, Roth EA, Markwald RR. 2003. Cell and organ printing 2: fusion of cell  
19 aggregates in three-dimensional gels. *Anat Rec A Discov Mol Cell Evol Biol* 272(2):497-502.
- 20 Burdett E, Kasper FK, Mikos AG, Ludwig JA. 2010. Engineering tumors: a tissue engineering perspective in  
21 cancer biology. *Tissue Eng Part B Rev* 16(3):351-9.
- 22 Cavnar SP, Salomonsson E, Luker KE, Luker GD, Takayama S. 2014. Transfer, imaging, and analysis plate for  
23 facile handling of 384 hanging drop 3D tissue spheroids. *J Lab Autom* 19(2):208-14.
- 24 Colombini A, Ceriani C, Banfi G, Brayda-Bruno M, Moretti M. 2014a. Fibrin in Intervertebral Disc Tissue  
25 Engineering. *Tissue Eng Part B Rev*.
- 26 Colombini A, Lopa S, Ceriani C, Lovati A, Croiset S, Di Giancamillo A, Lombardi G, Banfi G, Moretti M. 2014b.  
27 In vitro characterization and in vivo behavior of human nucleus pulposus and annulus fibrosus cells  
28 in clinical grade fibrin and collagen-enriched fibrin gels. *Tissue Eng Part A*:In press.
- 29 Cui X, Boland T. 2009. Human microvasculature fabrication using thermal inkjet printing technology.  
30 *Biomaterials* 30(31):6221-7.
- 31 de Ridder L, Cornelissen M, de Ridder D. 2000. Autologous spheroid culture: a screening tool for human  
32 brain tumour invasion. *Crit Rev Oncol Hematol* 36(2-3):107-22.
- 33 Dehne T, Schenk R, Perka C, Morawietz L, Pruss A, Sittinger M, Kaps C, Ringe J. 2010. Gene expression  
34 profiling of primary human articular chondrocytes in high-density micromasses reveals patterns of  
35 recovery, maintenance, re- and dedifferentiation. *Gene* 462(1-2):8-17.
- 36 Fennema E, Rivron N, Rouwkema J, van Blitterswijk C, de Boer J. 2013. Spheroid culture as a tool for  
37 creating 3D complex tissues. *Trends Biotechnol* 31(2):108-15.
- 38 Fu CY, Tseng SY, Yang SM, Hsu L, Liu CH, Chang HY. 2014. A microfluidic chip with a U-shaped  
39 microstructure array for multicellular spheroid formation, culturing and analysis. *Biofabrication*  
40 6(1):015009.
- 41 Gerberich BG, Bhatia SK. 2013. Tissue scaffold surface patterning for clinical applications. *Biotechnol J*  
42 8(1):73-84.
- 43 Giannoni P, Cancedda R. 2006. Articular chondrocyte culturing for cell-based cartilage repair: needs and  
44 perspectives. *Cells Tissues Organs* 184(1):1-15.
- 45 Giannoni P, Pagano A, Maggi E, Arbico R, Randazzo N, Grandizio M, Cancedda R, Dozin B. 2005. Autologous  
46 chondrocyte implantation (ACI) for aged patients: development of the proper cell expansion  
47 conditions for possible therapeutic applications. *Osteoarthritis Cartilage* 13(7):589-600.
- 48 Giovannini S, Diaz-Romero J, Aigner T, Heini P, Mainil-Varlet P, Nestic D. 2010. Micromass co-culture of  
49 human articular chondrocytes and human bone marrow mesenchymal stem cells to investigate  
50 stable neocartilage tissue formation in vitro. *Eur Cell Mater* 20:245-59.

1 Gomez-Sjoberg R, Leyrat AA, Houseman BT, Shokat K, Quake SR. 2010. Biocompatibility and reduced drug  
2 absorption of sol-gel-treated poly(dimethyl siloxane) for microfluidic cell culture applications. *Anal*  
3 *Chem* 82(21):8954-60.

4 Harris CA, Resau JH, Hudson EA, West RA, Moon C, Black AD, McAllister JP, 2nd. 2011. Reduction of protein  
5 adsorption and macrophage and astrocyte adhesion on ventricular catheters by polyethylene glycol  
6 and N-acetyl-L-cysteine. *J Biomed Mater Res A* 98(3):425-33.

7 Higuera GA, Hendriks JA, van Dalum J, Wu L, Schotel R, Moreira-Teixeira L, van den Doel M, Leijten JC,  
8 Riesle J, Karperien M and others. 2013. In vivo screening of extracellular matrix components  
9 produced under multiple experimental conditions implanted in one animal. *Integr Biol (Camb)*  
10 5(6):889-98.

11 Hildner F, Concaro S, Peterbauer A, Wolbank S, Danzer M, Lindahl A, Gatenholm P, Redl H, van Griensven  
12 M. 2009. Human adipose-derived stem cells contribute to chondrogenesis in coculture with human  
13 articular chondrocytes. *Tissue Eng Part A* 15(12):3961-9.

14 Hsu SM, Raine L, Fanger H. 1981. Use of avidin-biotin-peroxidase complex (ABC) in immunoperoxidase  
15 techniques: a comparison between ABC and unlabeled antibody (PAP) procedures. *J Histochem*  
16 *Cytochem* 29(4):577-80.

17 Huang B, Wu H, Kim S, Zare RN. 2005. Coating of poly(dimethylsiloxane) with n-dodecyl-beta-D-maltoside  
18 to minimize nonspecific protein adsorption. *Lab Chip* 5(10):1005-7.

19 Hwang CM, Ay B, Kaplan DL, Rubin JP, Marra KG, Atala A, Yoo JJ, Lee SJ. 2013. Assessments of injectable  
20 alginate particle-embedded fibrin hydrogels for soft tissue reconstruction. *Biomed Mater*  
21 8(1):014105.

22 Jakab K, Neagu A, Mironov V, Forgacs G. 2004. Organ printing: fiction or science. *Biorheology* 41(3-4):371-5.

23 Jakob M, Demarteau O, Schafer D, Hintermann B, Dick W, Heberer M, Martin I. 2001. Specific growth  
24 factors during the expansion and redifferentiation of adult human articular chondrocytes enhance  
25 chondrogenesis and cartilaginous tissue formation in vitro. *J Cell Biochem* 81(2):368-77.

26 Kolesky DB, Truby RL, Gladman AS, Busbee TA, Homan KA, Lewis JA. 2014. 3D bioprinting of vascularized,  
27 heterogeneous cell-laden tissue constructs. *Adv Mater* 26(19):3124-30.

28 Koroleva A, Gittard S, Schlie S, Deiwick A, Jockenhoevel S, Chichkov B. 2012. Fabrication of fibrin scaffolds  
29 with controlled microscale architecture by a two-photon polymerization-micromolding technique.  
30 *Biofabrication* 4(1):015001.

31 Lagana M, Arrigoni C, Lopa S, Sansone V, Zagra L, Moretti M, Raimondi MT. 2014. Characterization of  
32 articular chondrocytes isolated from 211 osteoarthritic patients. *Cell Tissue Bank* 15(1):59-66.

33 Lopa S, Colombini A, Sansone V, Preis FW, Moretti M. 2013. Influence on chondrogenesis of human  
34 osteoarthritic chondrocytes in co-culture with donor-matched mesenchymal stem cells from  
35 infrapatellar fat pad and subcutaneous adipose tissue. *Int J Immunopathol Pharmacol* 26(1  
36 Suppl):23-31.

37 Lopa S, Colombini A, Stanco D, de Girolamo L, Sansone V, Moretti M. 2014. Donor-matched mesenchymal  
38 stem cells from knee infrapatellar and subcutaneous adipose tissue of osteoarthritic donors display  
39 differential chondrogenic and osteogenic commitment. *Eur Cell Mater* 27:298-311.

40 Mauck RL, Wang CC, Oswald ES, Ateshian GA, Hung CT. 2003. The role of cell seeding density and nutrient  
41 supply for articular cartilage tissue engineering with deformational loading. *Osteoarthritis Cartilage*  
42 11(12):879-90.

43 Meinhart J, Fussenegger M, Hobling W. 1999. Stabilization of fibrin-chondrocyte constructs for cartilage  
44 reconstruction. *Ann Plast Surg* 42(6):673-8.

45 Mironov V, Visconti RP, Kasyanov V, Forgacs G, Drake CJ, Markwald RR. 2009. Organ printing: tissue  
46 spheroids as building blocks. *Biomaterials* 30(12):2164-74.

47 Moreira Teixeira LS, Leijten JC, Sobral J, Jin R, van Apeldoorn AA, Feijen J, van Blitterswijk C, Dijkstra PJ,  
48 Karperien M. 2012. High throughput generated micro-aggregates of chondrocytes stimulate  
49 cartilage formation in vitro and in vivo. *Eur Cell Mater* 23:387-99.

50 Murphy SV, Atala A. 2014. 3D bioprinting of tissues and organs. *Nat Biotechnol* 32(8):773-85.

51 Napolitano AP, Chai P, Dean DM, Morgan JR. 2007. Dynamics of the self-assembly of complex cellular  
52 aggregates on micromolded nonadhesive hydrogels. *Tissue Eng* 13(8):2087-94.

- 1 Patra B, Chen YH, Peng CC, Lin SC, Lee CH, Tung YC. 2013. A microfluidic device for uniform-sized cell  
2 spheroids formation, culture, harvesting and flow cytometry analysis. *Biomicrofluidics* 7(5):54114.
- 3 Peretti GM, Randolph MA, Villa MT, Buragas MS, Yaremchuk MJ. 2000. Cell-based tissue-engineered  
4 allogeneic implant for cartilage repair. *Tissue Eng* 6(5):567-76.
- 5 Piraino F, Selimovic S, Adamo M, Pero A, Manoucheri S, Bok Kim S, Demarchi D, Khademhosseini A. 2012.  
6 Polyester -assay chip for stem cell studies. *Biomicrofluidics* 6(4):44109.
- 7 Ratnayaka SH, Hillburn TE, Forouzan O, Shevkoplyas SS, Khismatullin DB. 2013. PDMS well platform for  
8 culturing millimeter-size tumor spheroids. *Biotechnol Prog* 29(5):1265-9.
- 9 Sabatino MA, Santoro R, Gueven S, Jaquier C, Wendt DJ, Martin I, Moretti M, Barbero A. 2012. Cartilage  
10 graft engineering by co-culturing primary human articular chondrocytes with human bone marrow  
11 stromal cells. *J Tissue Eng Regen Med*.
- 12 Schulze-Tanzil G. 2009. Activation and dedifferentiation of chondrocytes: implications in cartilage injury and  
13 repair. *Ann Anat* 191(4):325-38.
- 14 Schuurman W, Khristov V, Pot MW, van Weeren PR, Dhert WJ, Malda J. 2011. Bioprinting of hybrid tissue  
15 constructs with tailorable mechanical properties. *Biofabrication* 3(2):021001.
- 16 Scotti C, Mangiavini L, Boschetti F, Vitari F, Domeneghini C, Frascini G, Peretti GM. 2010. Effect of in vitro  
17 culture on a chondrocyte-fibrin glue hydrogel for cartilage repair. *Knee Surg Sports Traumatol*  
18 *Arthrosc* 18(10):1400-6.
- 19 Selimovic S, Piraino F, Bae H, Rasponi M, Redaelli A, Khademhosseini A. 2011. Microfabricated polyester  
20 conical microwells for cell culture applications. *Lab Chip* 11(14):2325-32.
- 21 Steinert AF, Ghivizzani SC, Rethwilm A, Tuan RS, Evans CH, Noth U. 2007. Major biological obstacles for  
22 persistent cell-based regeneration of articular cartilage. *Arthritis Res Ther* 9(3):213.
- 23 Talukdar S, Nguyen QT, Chen AC, Sah RL, Kundu SC. 2011. Effect of initial cell seeding density on 3D-  
24 engineered silk fibroin scaffolds for articular cartilage tissue engineering. *Biomaterials* 32(34):8927-  
25 37.
- 26 Toepke MW, Beebe DJ. 2006. PDMS absorption of small molecules and consequences in microfluidic  
27 applications. *Lab Chip* 6(12):1484-6.
- 28 Tung YC, Hsiao AY, Allen SG, Torisawa YS, Ho M, Takayama S. 2011. High-throughput 3D spheroid culture  
29 and drug testing using a 384 hanging drop array. *Analyst* 136(3):473-8.
- 30 Whitesides GM, Ostuni E, Takayama S, Jiang X, Ingber DE. 2001. Soft lithography in biology and  
31 biochemistry. *Annu Rev Biomed Eng* 3:335-73.
- 32 Wolbank S, Pichler V, Ferguson JC, Meinel A, van Griensven M, Goppelt A, Redl H. 2014. Non-invasive in vivo  
33 tracking of fibrin degradation by fluorescence imaging. *J Tissue Eng Regen Med*.
- 34 Wolf F, Candrian C, Wendt D, Farhadi J, Heberer M, Martin I, Barbero A. 2008. Cartilage tissue engineering  
35 using pre-aggregated human articular chondrocytes. *Eur Cell Mater* 16:92-9.
- 36 Wu L, Prins HJ, Helder MN, van Blitterswijk CA, Karperien M. 2012. Trophic effects of mesenchymal stem  
37 cells in chondrocyte co-cultures are independent of culture conditions and cell sources. *Tissue Eng*  
38 *Part A* 18(15-16):1542-51.
- 39 Xu F, Sridharan B, Wang S, Gurkan UA, Syverud B, Demirci U. 2011. Embryonic stem cell bioprinting for  
40 uniform and controlled size embryoid body formation. *Biomicrofluidics* 5(2):22207.
- 41 Zhang Z, McCaffery JM, Spencer RG, Francomano CA. 2004. Hyaline cartilage engineered by chondrocytes in  
42 pellet culture: histological, immunohistochemical and ultrastructural analysis in comparison with  
43 cartilage explants. *J Anat* 205(3):229-37.
- 44 Zinchenko YS, Coger RN. 2005. Engineering micropatterned surfaces for the coculture of hepatocytes and  
45 Kupffer cells. *J Biomed Mater Res A* 75(1):242-8.

46

47



1 **List of Figures:**

2 **Figure 1. Fabrication of PDMS multi-well chips for cell spheroid generation and culture. (a)**

3 Laser-ablated PMMA molds (I) were used to generate the multi-well PDMS chips (II). PDMS chips  
4 were placed in a 12 well multiwell plate, cells were seeded in the wells and the multiplate was  
5 centrifuged to promote spheroid formation (III). Then, medium was added and PDMS chips were  
6 maintained in culture for 21 days (IV). **(b)** CAD drawing including top view with insets showing  
7 diameters, pitch, height of the wells and taper angle. Corresponding values for the two  
8 configurations (Chip A, Chip B) are indicated in table. **(c)** 3D rendering of Chip A and Chip B. **(d)**  
9 Optical images of chip A ( $\text{\O}_{\text{well}}$  2 mm) and chip B ( $\text{\O}_{\text{well}}$  3.4 mm) fabricated by PDMS replica  
10 molding on the corresponding PMMA master-templates (scale bars 1 mm, except where noted).

11

12 **Figure 2. Biofabrication of implantable multi-well fibrin constructs. (a)** Laser-ablated PMMA

13 molds (I) were used to generate PDMS counter-molds (II). Cells were mixed with fibrinogen and  
14 thrombin and poured into the PDMS mold to generate the multi-well bottom layer (III). After  
15 polymerization, the bottom layer was removed from the PDMS mold and cells were seeded in the  
16 wells of the construct (IV). A top layer made from cell-loaded fibrin was poured over the bottom  
17 layer to ultimate the scaffold (V). Medium was added for construct culture (VI). **(b)** CAD drawing  
18 including top view with insets showing diameters, pitch and height of the pillars. Corresponding  
19 values for the three mold configurations (Mold X, Mold Y, Mold Z) are indicated in table. **(c)** 3D  
20 rendering of the three PDMS mold configurations. **(d)** Top view of the three different bottom layer  
21 configurations of PMMA master templates and PDMS molds fabricated by laser ablation and  
22 replica molding, respectively (scale bars 5 mm).

23

24 **Figure 3. Validation of PDMS chips for formation and culture of cell spheroids. (a)** Scan of a

25 12 well multiwell plate containing PDMS multi-well chips after cell seeding (scale bar 10 mm). **(b-**  
26 **c)** Measurements of time required to perform cell seeding and medium refresh. **(d)** Micrographs of a

1 representative well of chip A and chip B at different time points after cell seeding (4 hours, 24  
2 hours, 21 days, scale bar 1 mm). (e) Average area of spheroids cultured in Chip A and Chip B over  
3 time (n=54, data obtained from 3 independent chips both for configuration A and B). (f-h)  
4 Metabolic activity, DNA content, and metabolic activity normalized on DNA measured in spheroids  
5 cultured for 21 days in standard conditions (n=9) or in PDMS chips (n=9, 9 samples harvested from  
6 3 independent chips both for configuration A and B). (i-j) Histological evaluation of GAGs and  
7 type II collagen deposition in spheroids cultured for 21 days in standard conditions and in PDMS  
8 chips (scale bars 200  $\mu$ m).

9  
10 **Figure 4. Fabrication of multi-well fibrin constructs and evaluation of cell distribution.** (a)  
11 Design and stereomicroscope micrographs showing the three different bottom layer configurations  
12 (scale bars 1 mm). (b) Micrographs showing cell distribution in the multi-well fibrin constructs.  
13 Green-stained cells are embedded into the bottom layer, whereas red-stained cells are seeded into  
14 the wells (scale bar 1 mm). (c) Micrographs showing the central section of a cell-seeded fibrin  
15 constructs ( $\text{O}_{\text{well}}$  1.5 mm, h 1.5 mm, phase contrast and fluorescence microscopy, scale bar 1 mm).  
16 (d) Micrographs showing the multi-well pattern in the construct after the top layer polymerization.  
17 Green-stained cells are embedded into bottom and top layer and red-stained cells are seeded into the  
18 wells (scale bar 1 mm).

19  
20 **Figure 5. Comparison between fibrin constructs without and with wells.** (a) Representative  
21 pictures of fibrin constructs w/o wells and w/ wells (scale bar 2 mm). (b) Micrographs showing cell  
22 distribution in fibrin constructs w/o wells and w/ wells (scale bar 2 mm). (c) Hematoxylin/eosin  
23 staining of construct sections. The border of the well is indicated by a dotted line and cells  
24 distributed along the lower border of the well are indicated by arrows (scale bar 200  $\mu$ m). (d-e)  
25 DNA content and GAGs content normalized on DNA measured in fibrin constructs w/ and w/o  
26 wells after 7 days of *in vitro* culture (n=3). (f-i) Transcriptional levels of *SOX9*, *COL2A1*, *ACAN*,

1 and *COMP* evaluated in fibrin constructs w/ and w/o wells after 1 and 7 days of *in vitro* culture  
2 (n=4). Gene expression data are normalized on GAPDH using the delta Ct (dCt) method.

3

4 **Figure 6. Cell distribution and GAGs content after *in vivo* implantation in nude mice. (a)**

5 Micrographs showing fibrin constructs w/o and w/ wells seeded with red and/or green stained cells

6 prior and after subcutaneous implantation in nude mice (scale bar 1 mm). **(b)** GAGs content

7 normalized on construct wet weight measured in fibrin constructs w/o and w/ wells prior and after

8 subcutaneous implantation.

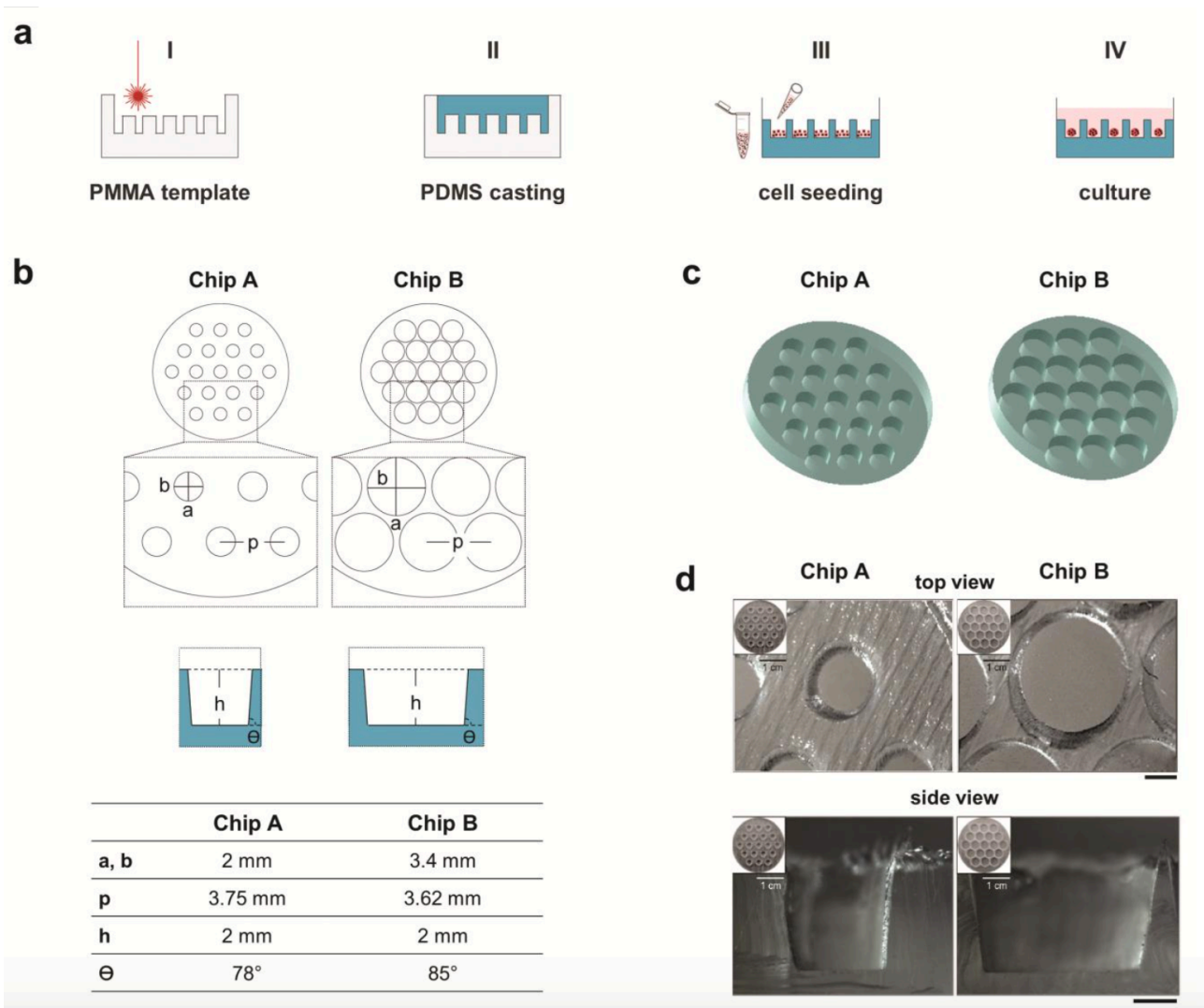


**Figure 1**

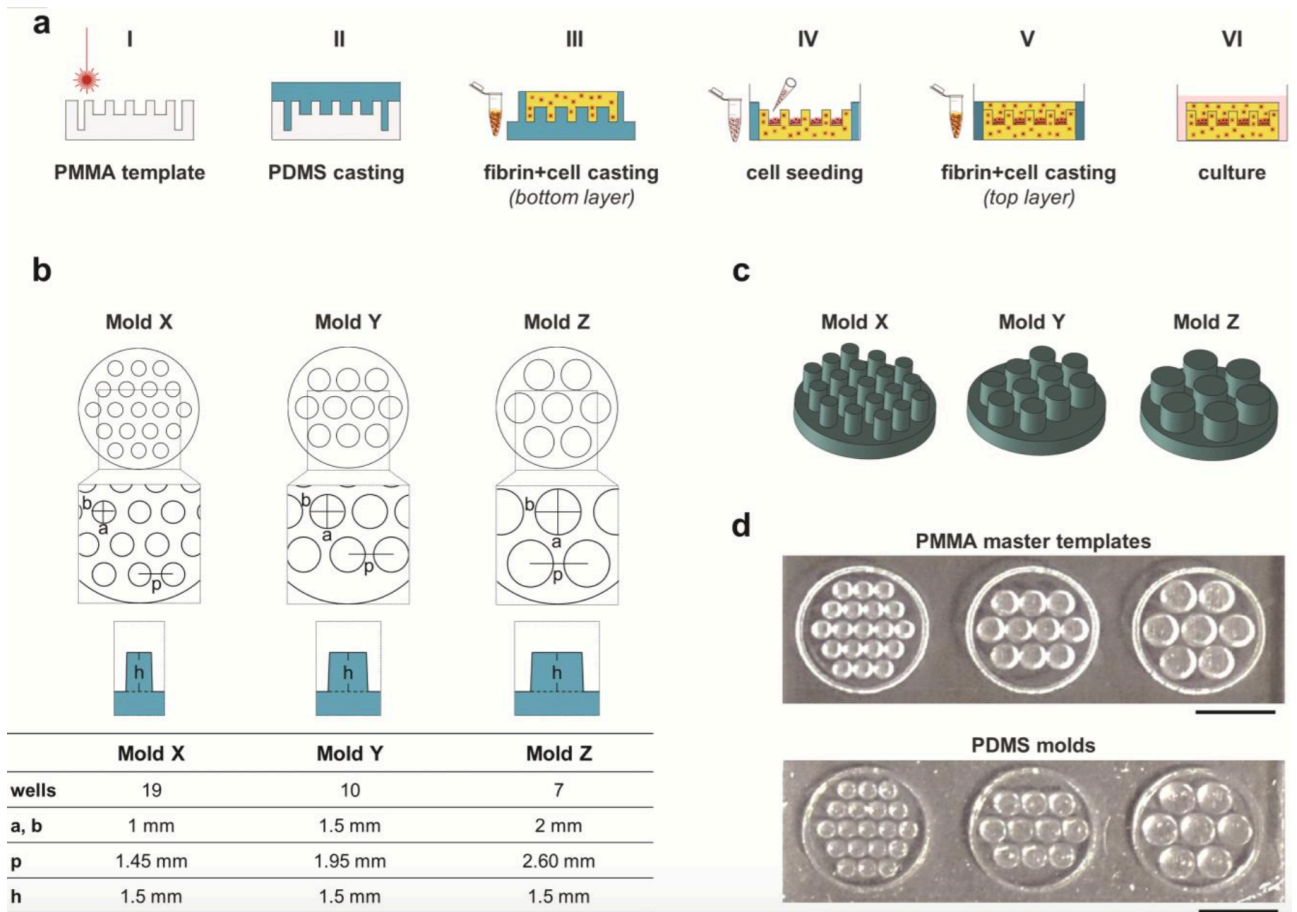


**Figure 2**

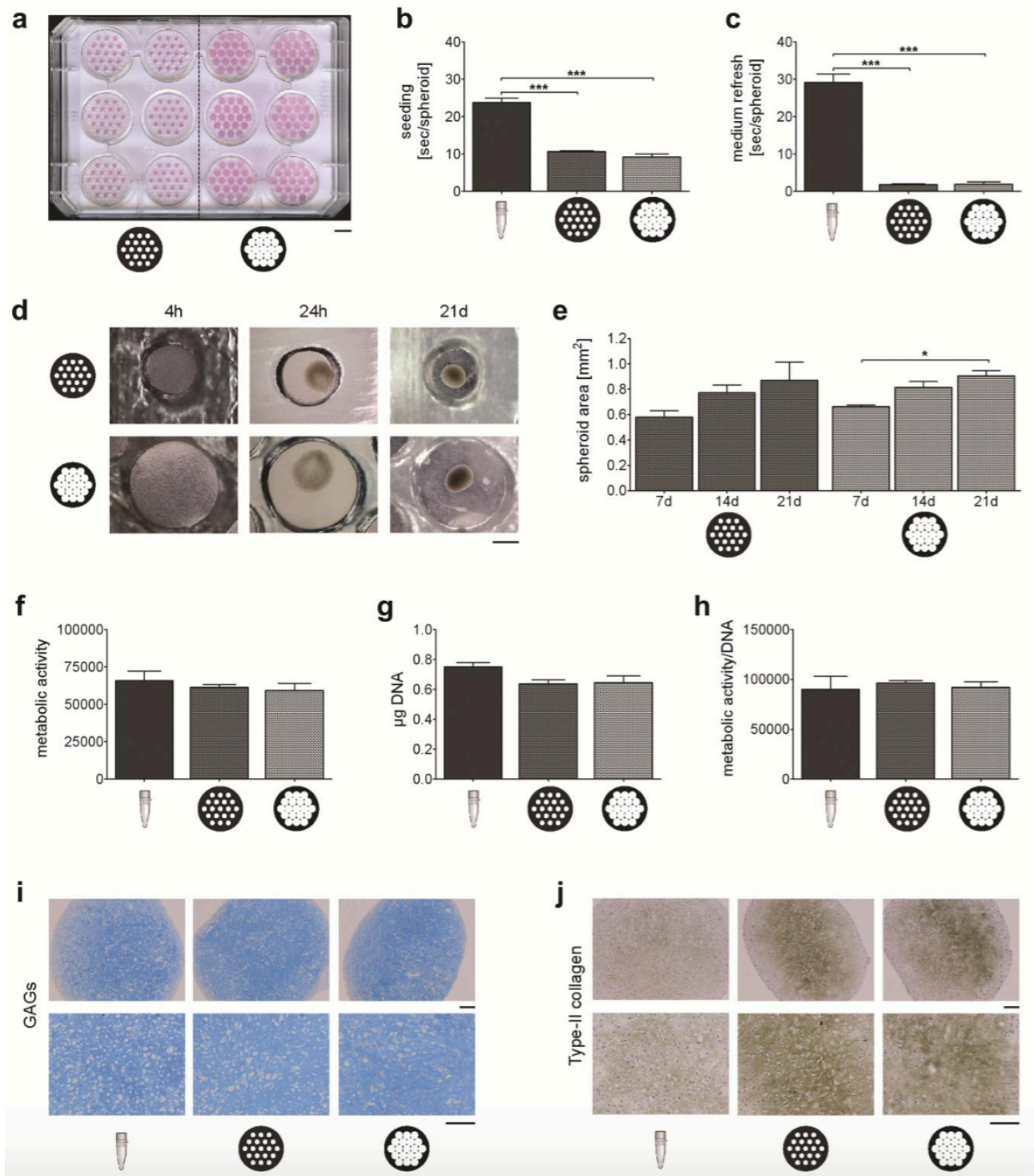


Figure 3

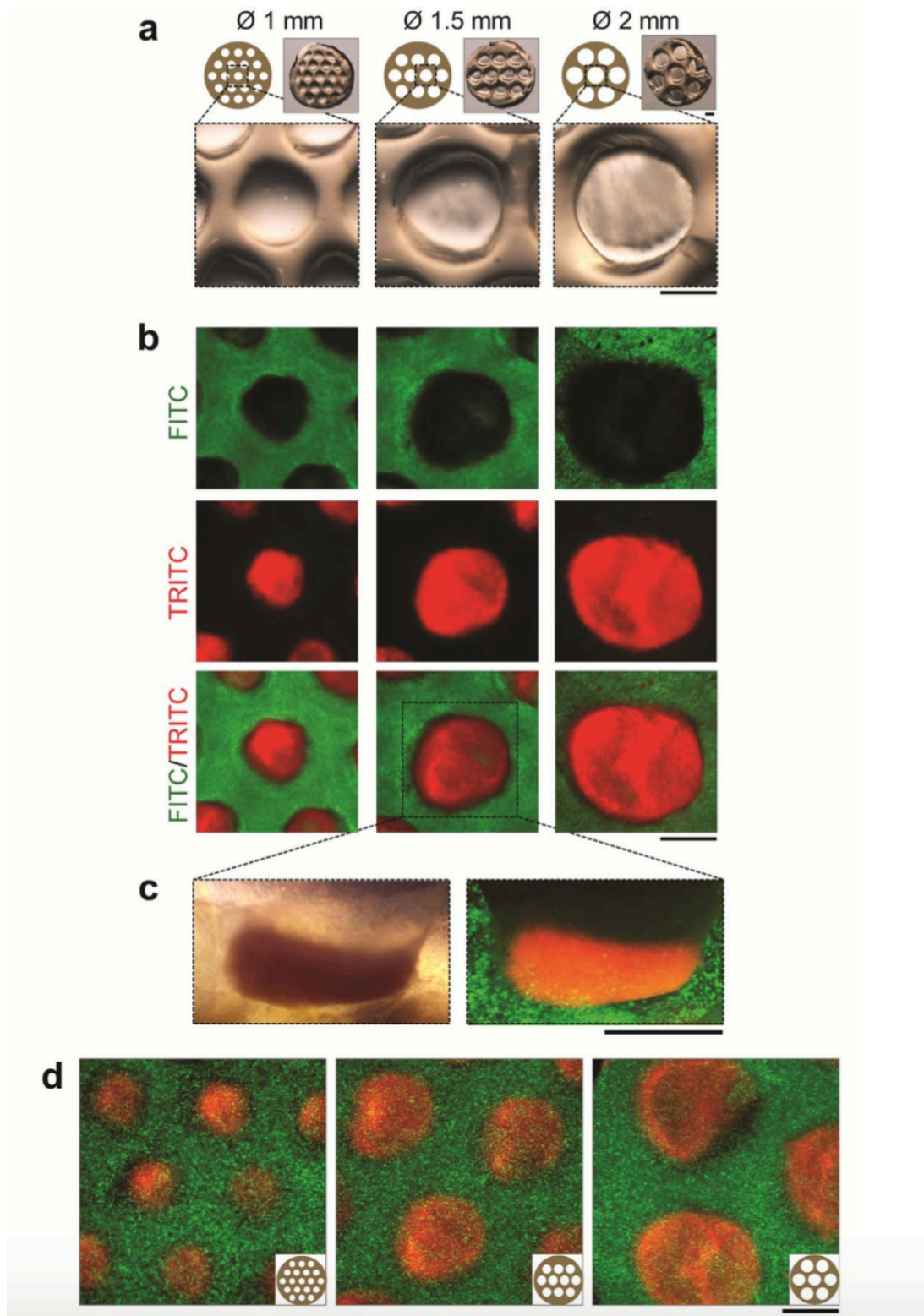
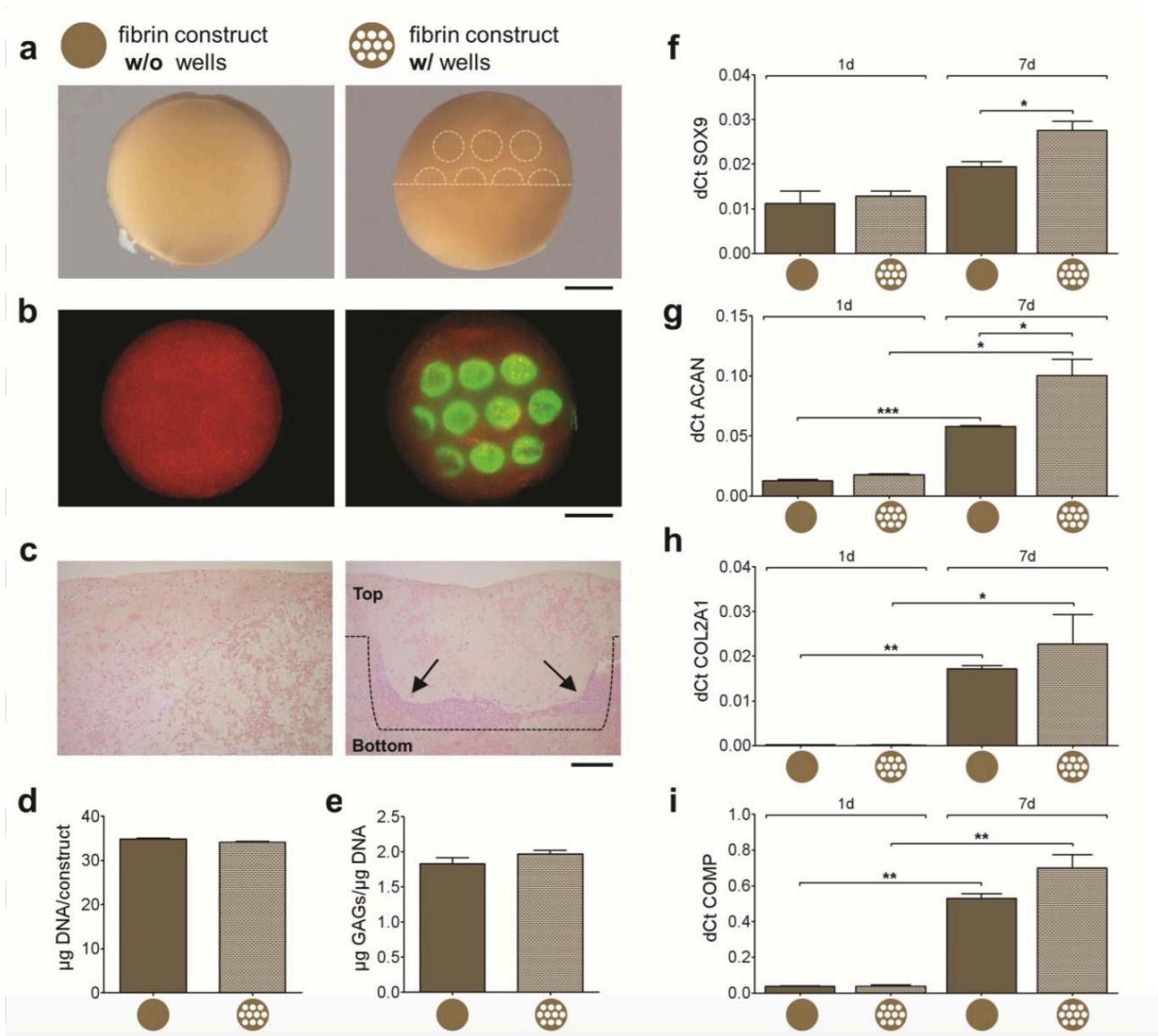
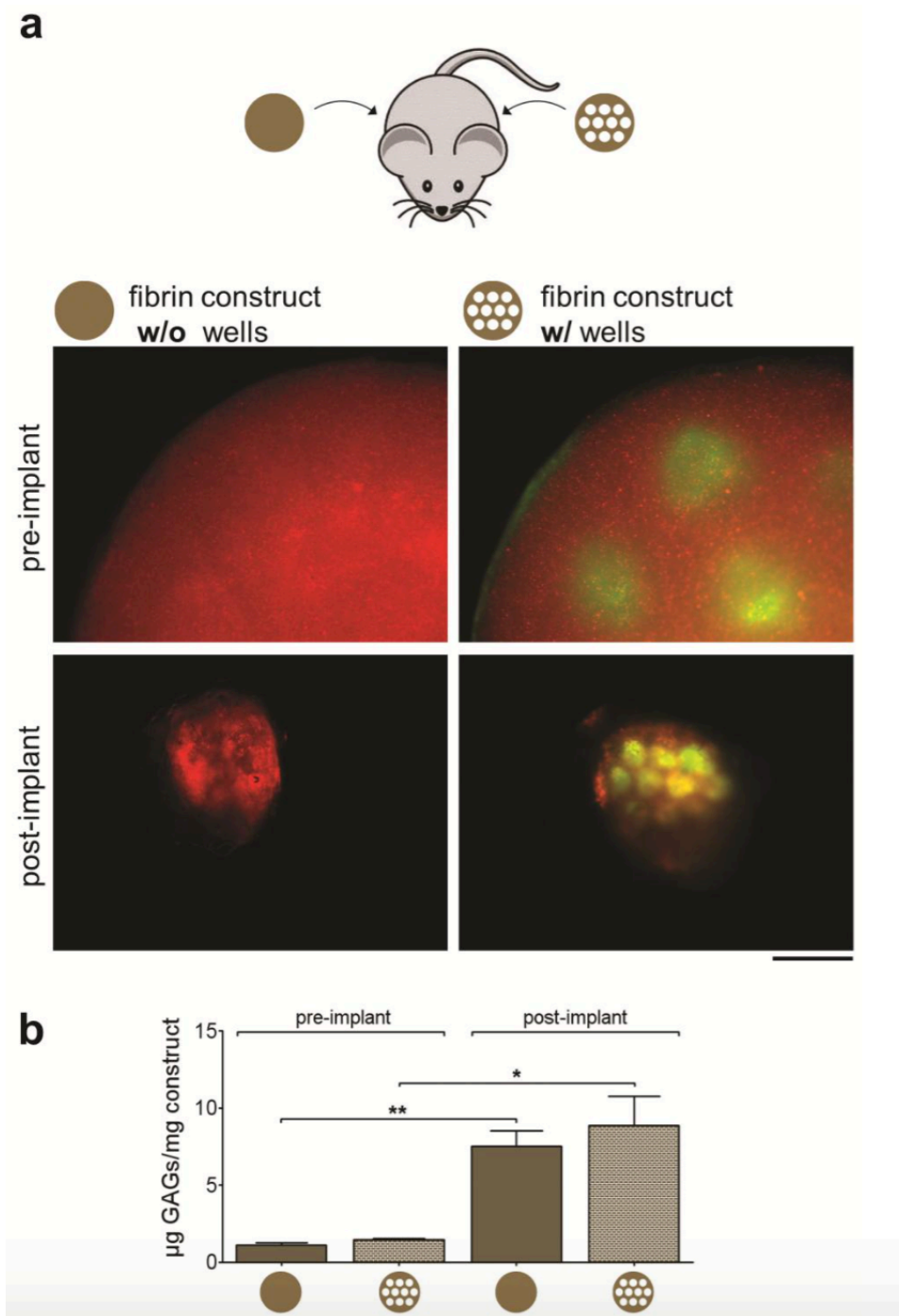


Figure 4



**Figure 5**





**Figure 6**